Gastrointestinal Tract

21

Plain Film

Plain films obtained in the supine position demonstrate the bowel gas pattern.

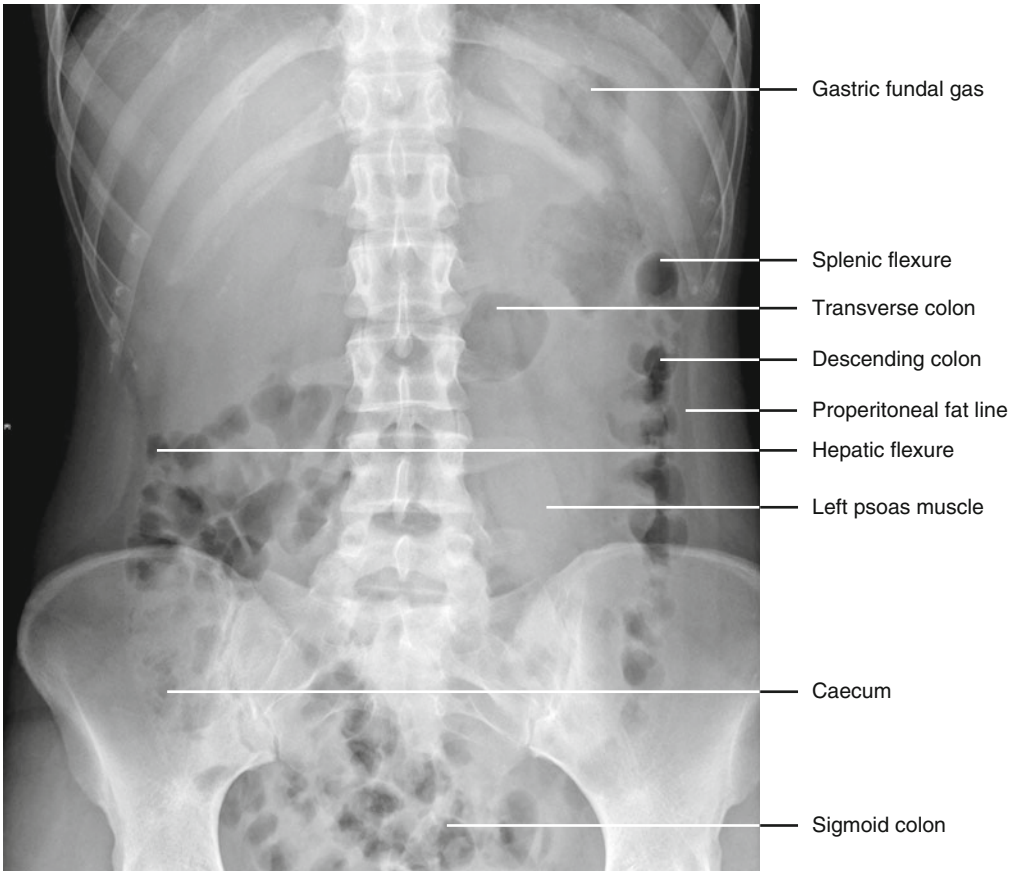

Fig. 21.1 Supine abdominal radiograph

S. Andronikou (ed.), *See Right Through Me*,
DOI 10.1007/978-3-642-23893-2_21, © Springer-Verlag Berlin Heidelberg 2012

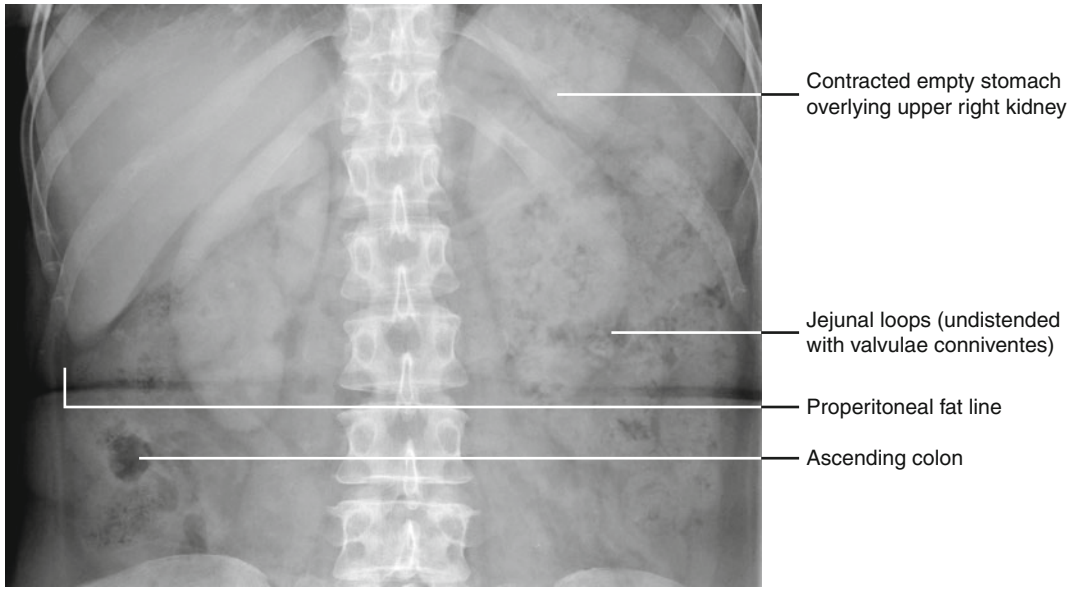

Fig. 21.2 Supine abdominal radiograph after IV contrast during an IVU

Pearl
Prone position for at least 5 min demonstrates the presence of rectal air.
The stomach is normally contracted or distended with food.
The duodenum is not visible.
Small bowel loops <3 cm in caliber are normal.
Maximum allowed caecal diameter is 9 and 5.5 cm for the rest of the colon.
An appendicolith may be visible in 7–15 % of the normal population.

Ultrasound

- Endoscopic ultrasound is used to assess mural anatomy.
- Transabdominal ultrasound may be used to assess gastro-esophageal reflux in children.
- The appendix is seen as a blind-ending tubular structure <6 mm in caliber.
- Anal sphincters can be optimally assessed using an endorectal probe.

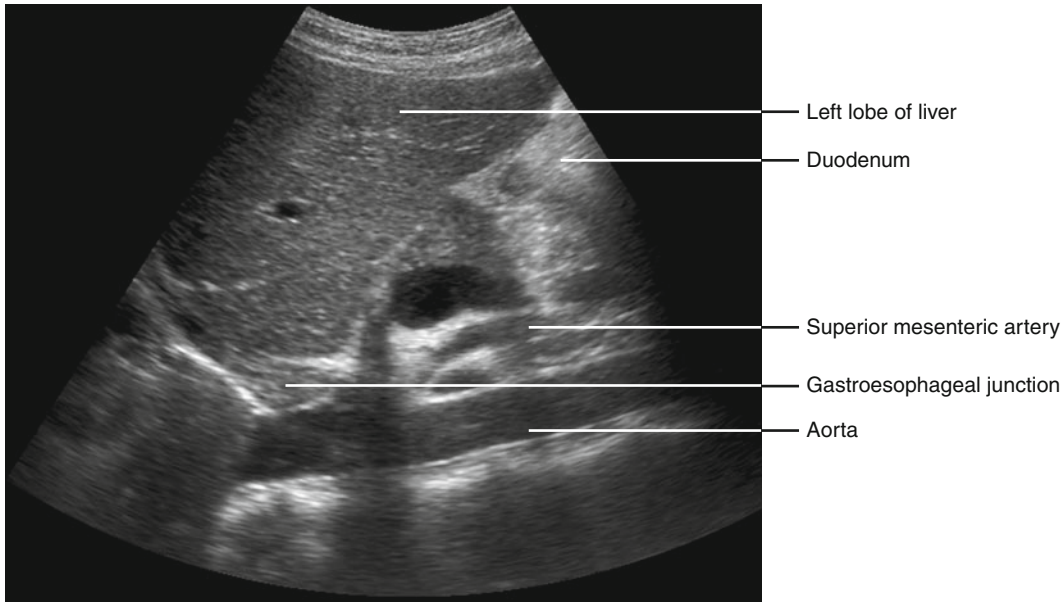

Fig. 21.3 Longitudinal ultrasound through the left lobe of the liver showing the gastroesophageal junction

Contrast Studies

Barium Meal

Assesses morphology and mucosal detail of stomach and duodenum. Usually performed with barium and air, hence called a double contrast barium meal (DCBM).

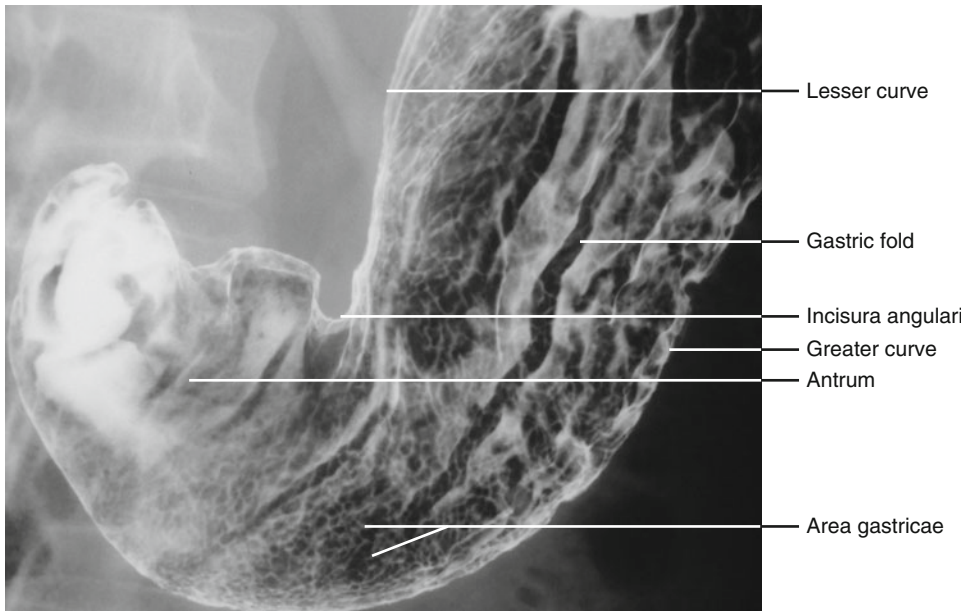

Fig. 21.4 DCBM of stomach

Pearl
Good coating and distension allows visualisation of the area gastricae and "see through" effect.

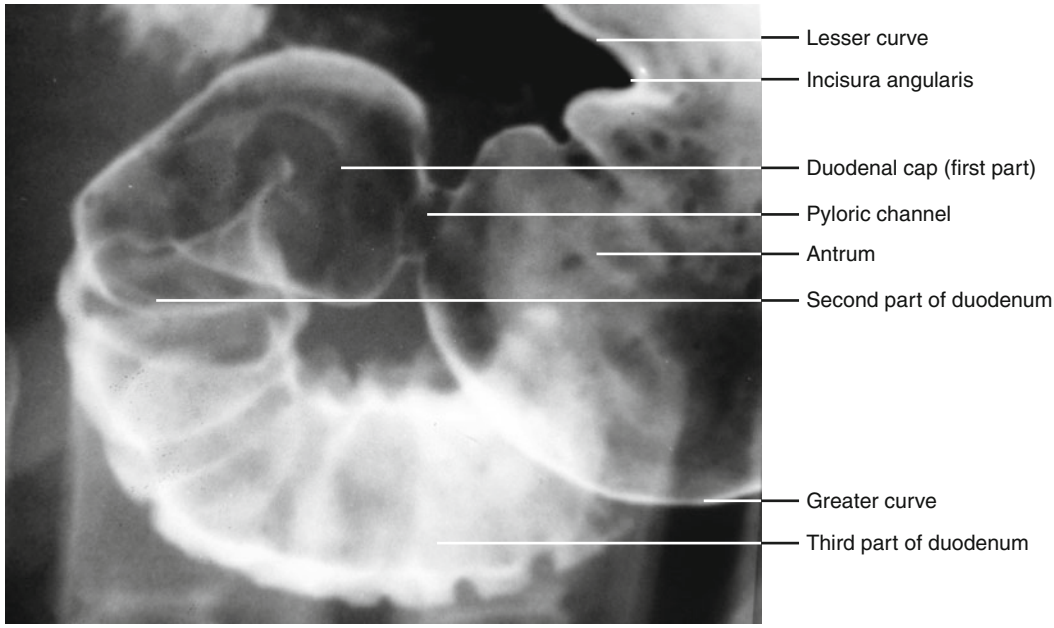

Fig. 21.5 DCBM of the duodenal cap

Pearl
The duodenal cap normally has the shape of a spade.
The duodenal cap may be indented by a normal gall bladder.

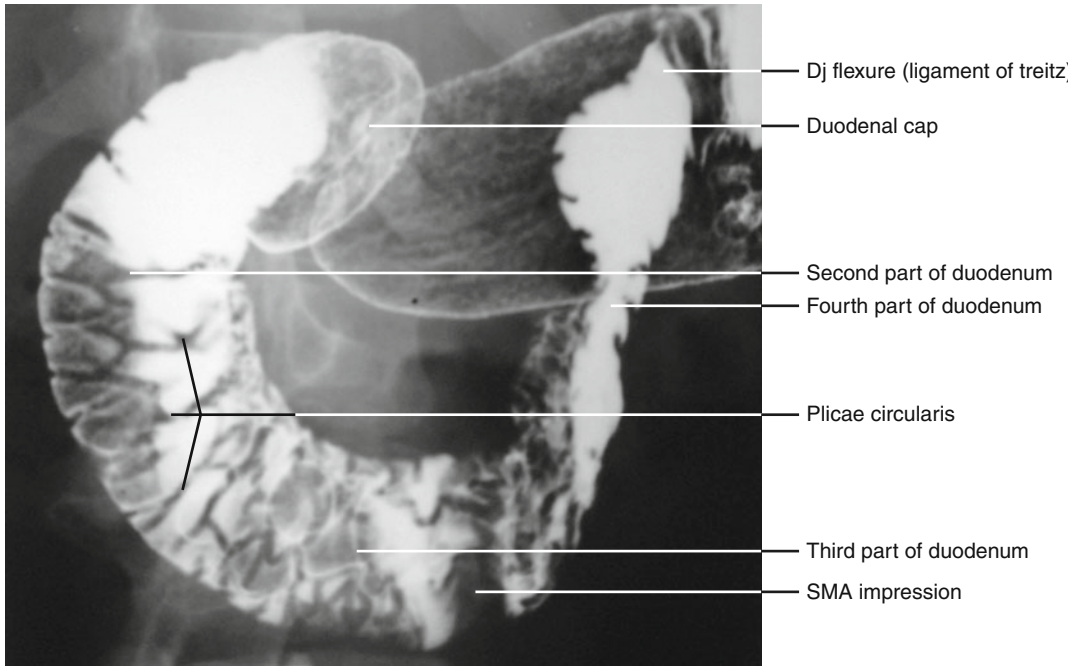

Fig. 21.6 DCBM of duodenum

Pearl
On the AP projection, D1 is located to the right of the spine and the duodeno-jejunal flexure to the left of the left pedicle at the same level or higher.
The major papilla is visualised in 66 % of cases.
The superior mesenteric artery may indent D3 (this may be pathological).

Small Bowel Enteroclysis

Demonstrates small bowel disposition, valvulae conniventes, and wall thickness.

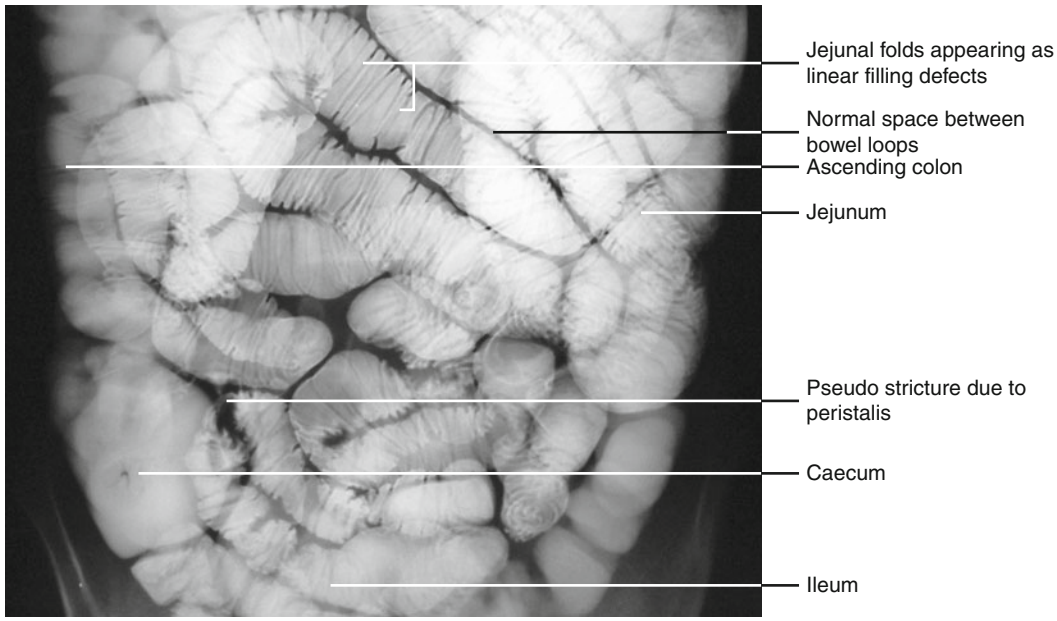

Fig. 21.7 Small bowel enteroclysis (SBE)

Pearl
Prominence of the valvulae conniventes at the jejunum.
Folds are smooth and <3 mm in thickness.
Bowel loops are evenly spaced.
Good contrast and exposure factors results in a "see-through" effect.

Barium Enema

Allows assessment of large bowl morphology and mucosal detail. Usually performed with barium and air and hence called a double contrast barium enema (DCBE).

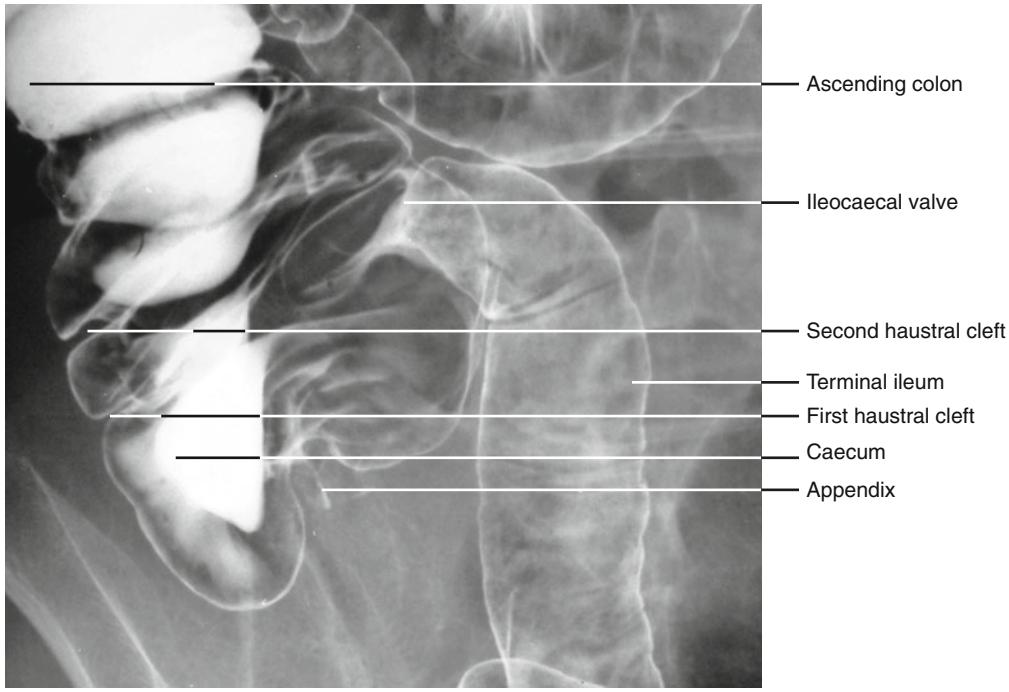

Fig. 21.8 DCBE of the caecum and terminal ileum with reflux into small bowel

Pearl
The normal terminal ileum resembles a "birds beak" at the ileocaecal valve.

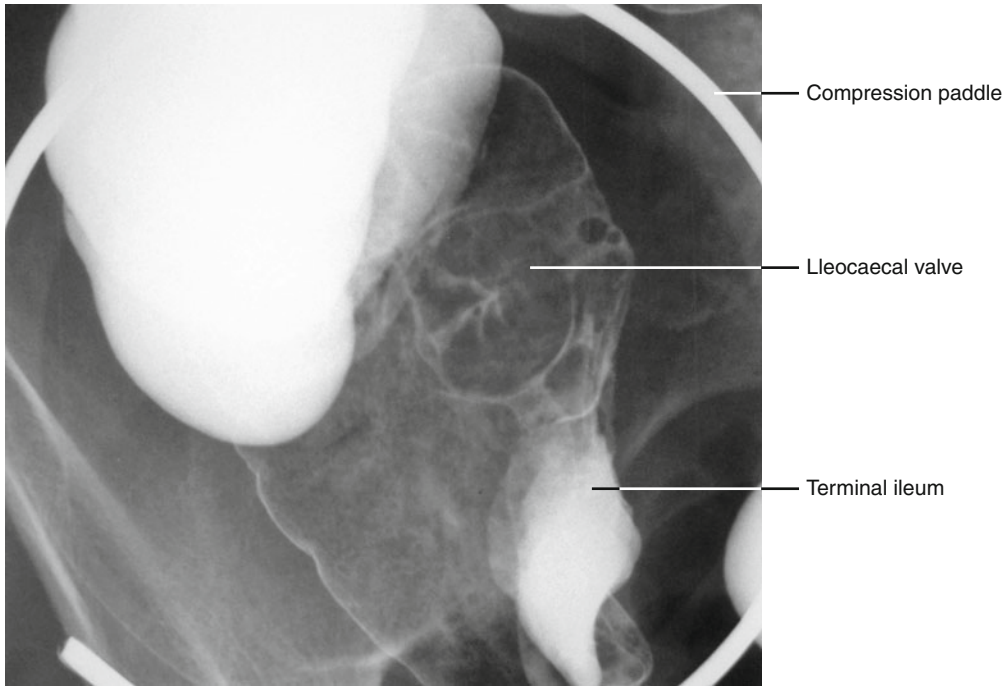

Fig. 21.9 DCBE with compression of the caecum

Pearl
A rounded filling defect in the caecum is caused by the ileocaecal valve.

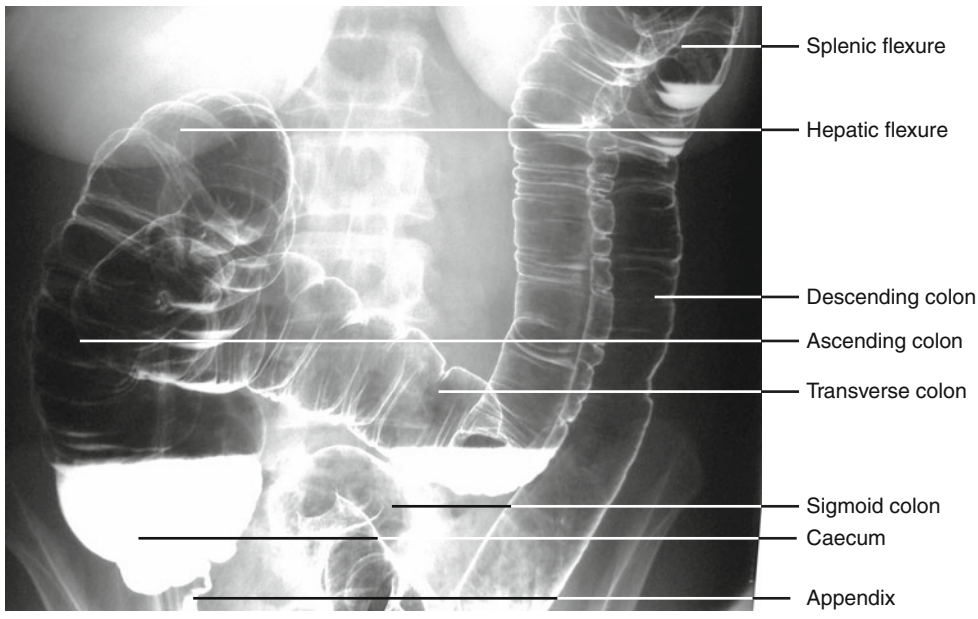

Fig. 21.10 DCBE of the large bowel, erect view

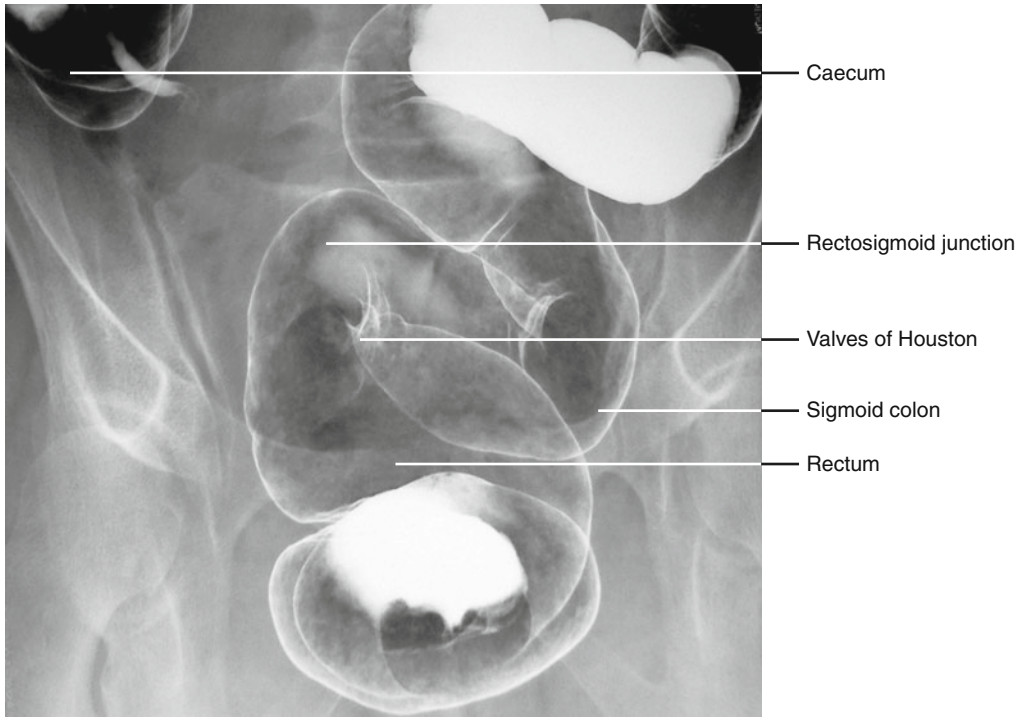

Fig. 21.11 DCBE of the rectosigmoid, AP view

Pearl
This view is performed prone "30° up" to elongate the bowel loops and the enema tube is removed to prevent obscuring of low lesions.

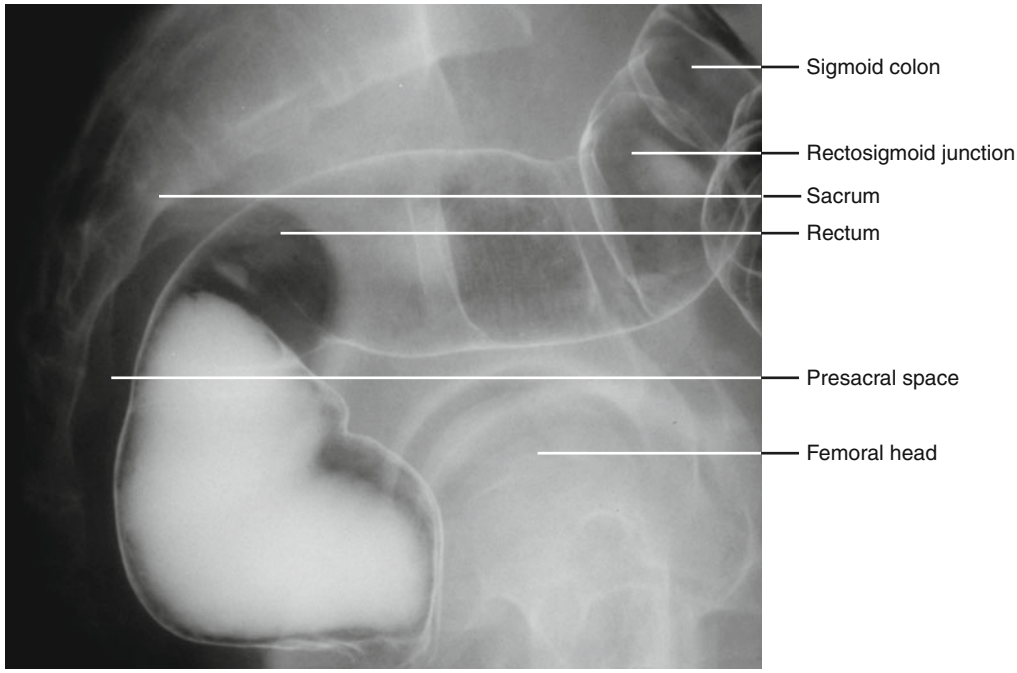

Fig. 21.12 DCBE of the rectosigmoid, AP view

Pearl
The normal presacral width is <15 mm at the fourth sacral element. This increases to 20 mm in obese and elderly patients.

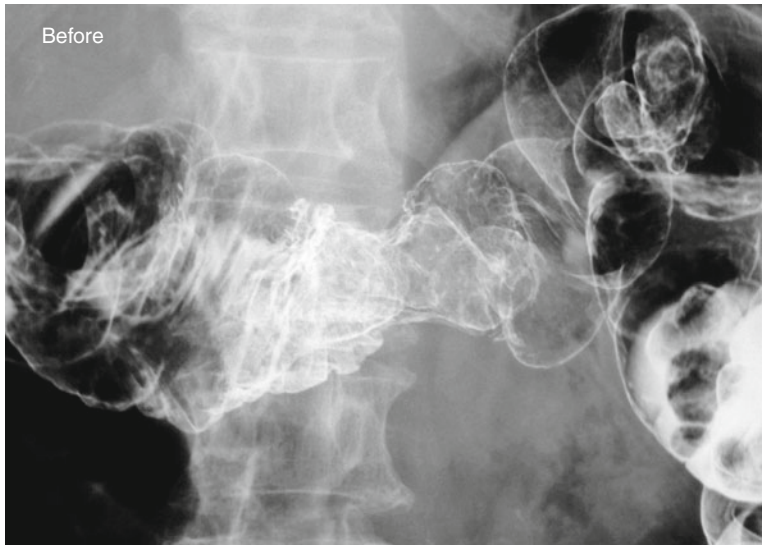

Fig. 21.13 Cannon's ring simulating pathology at the transverse colon during DCBE

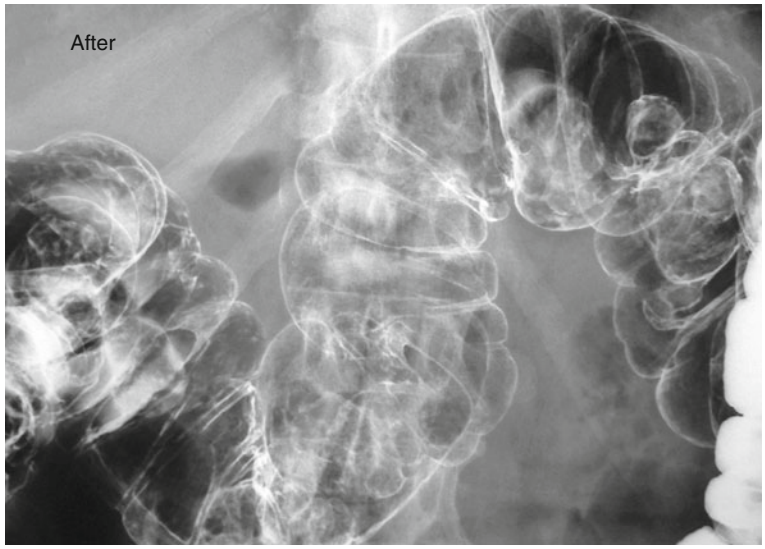

Fig. 21.14 IV muscle relaxant with air inflation demonstrates normal distensibility of the transverse colon at Cannon's ring

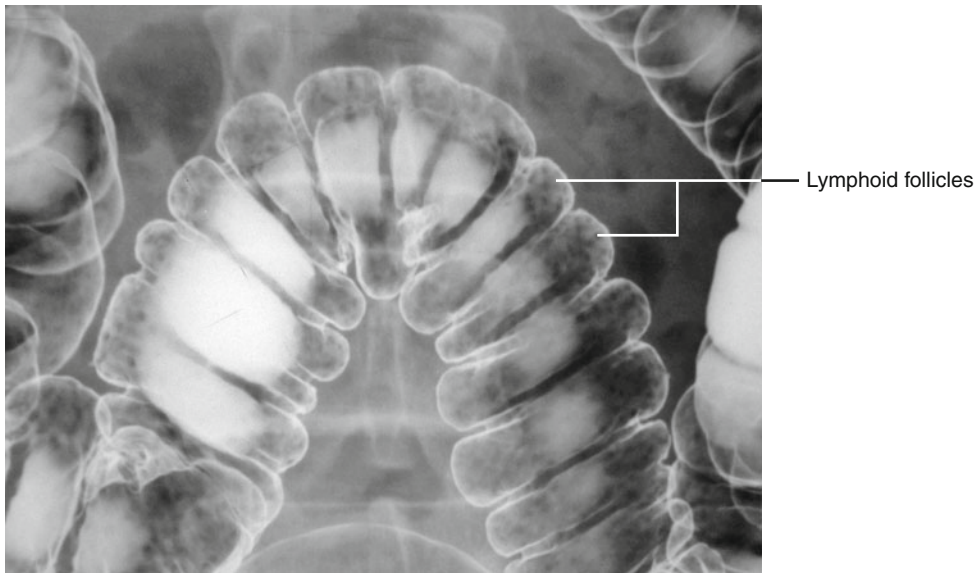

Fig. 21.15 DCBE demonstrating lymphoid follicles

Pearl
Lymphoid tissue aggregates are a normal variant and should measure <4 mm each.

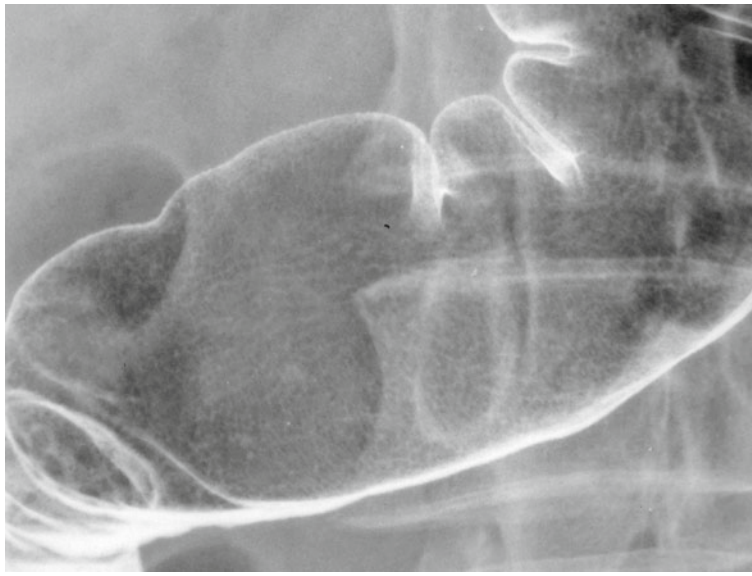

Fig. 21.16 DCBE demonstrating innominate lines

Pearl
These are superficial indentations of the mucosa due to the Crypts of Lieberkühn.

Computed Tomography

Optimal delineation of luminal, mural, and extramural anatomy.

Performed with positive/negative intraluminal contrast (using air, water or oral contrast agent).

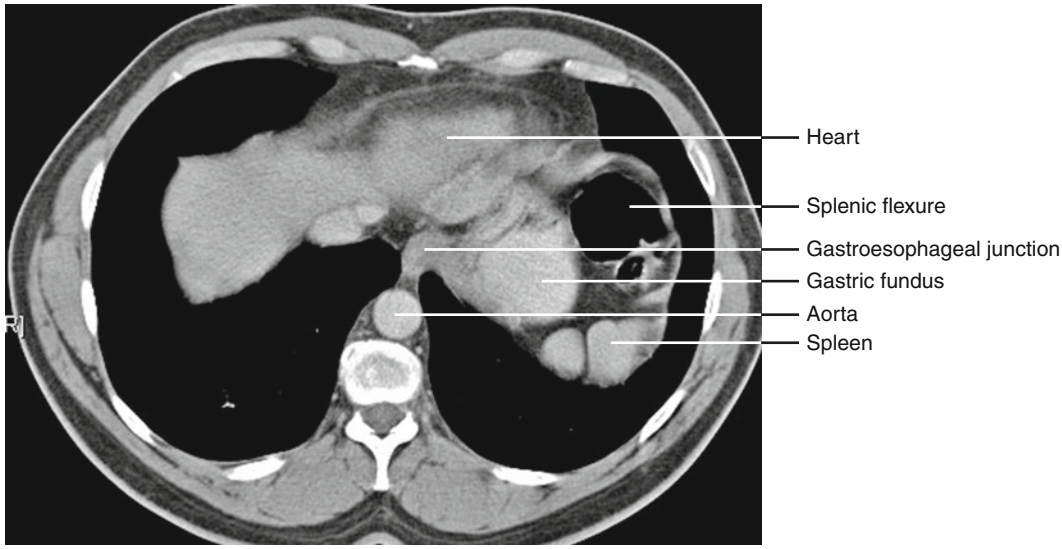

Fig. 21.17 Axial post contrast CT demonstrating the splenic flexure of the colon

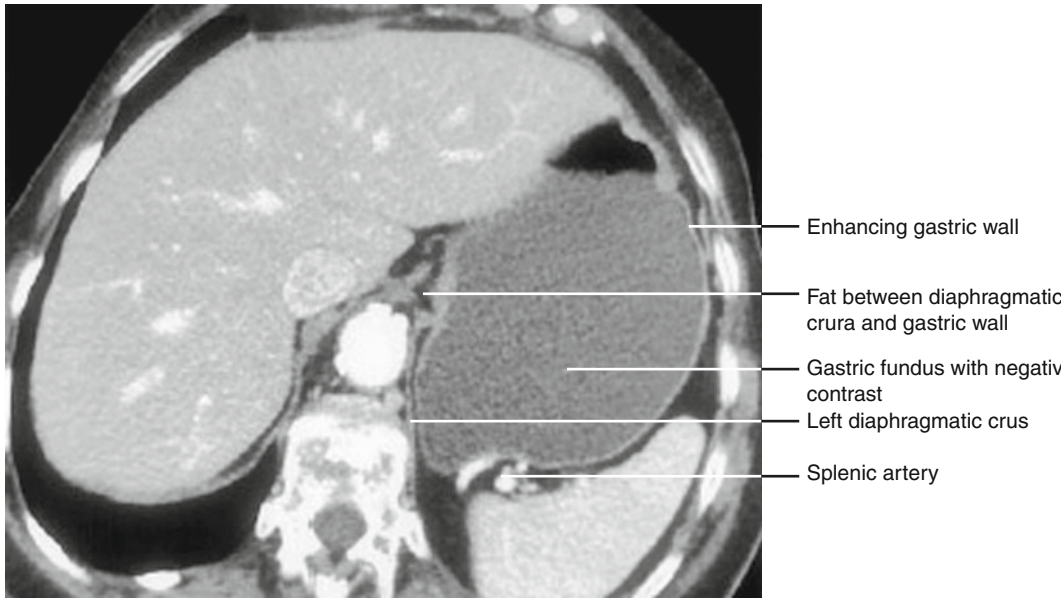

Fig. 21.18 Axial post contrast CT demonstrating the stomach fundus

Pearl
Thickness of the gastric wall is even except at the gastroesophageal junction.
Gastric wall is accentuated by negative intraluminal contrast and perigastric fat.
A fat plane separates the diaphragmatic crura from the gastric wall.

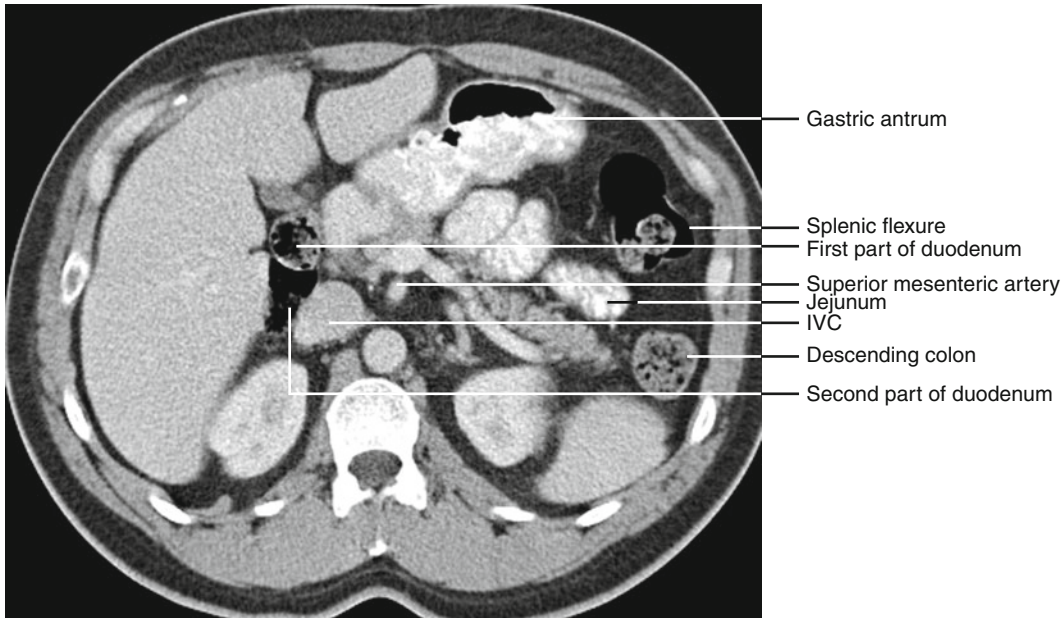

Fig. 21.19 Axial post contrast CT demonstrating the second part of the duodenum

Pearl
The superior mesenteric artery should always be surrounded by a cuff of fat.

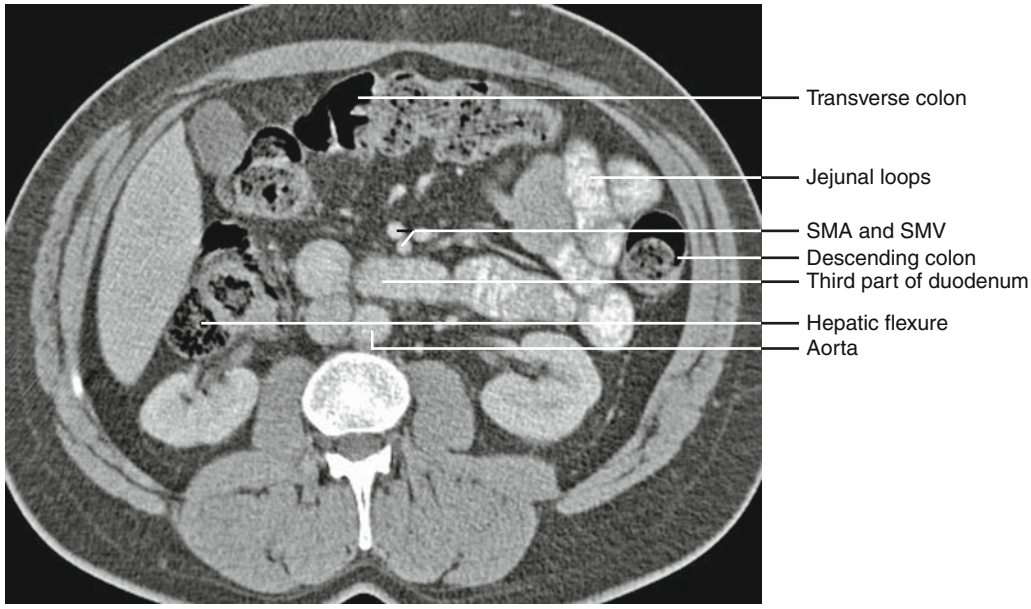

Fig. 21.20 Axial post contrast CT demonstrating the third part of the duodenum

Pearl
D3 is the last of the three structures passing between the SMA and the aorta. The other two are the uncinate process of the pancreas and the left renal vein.

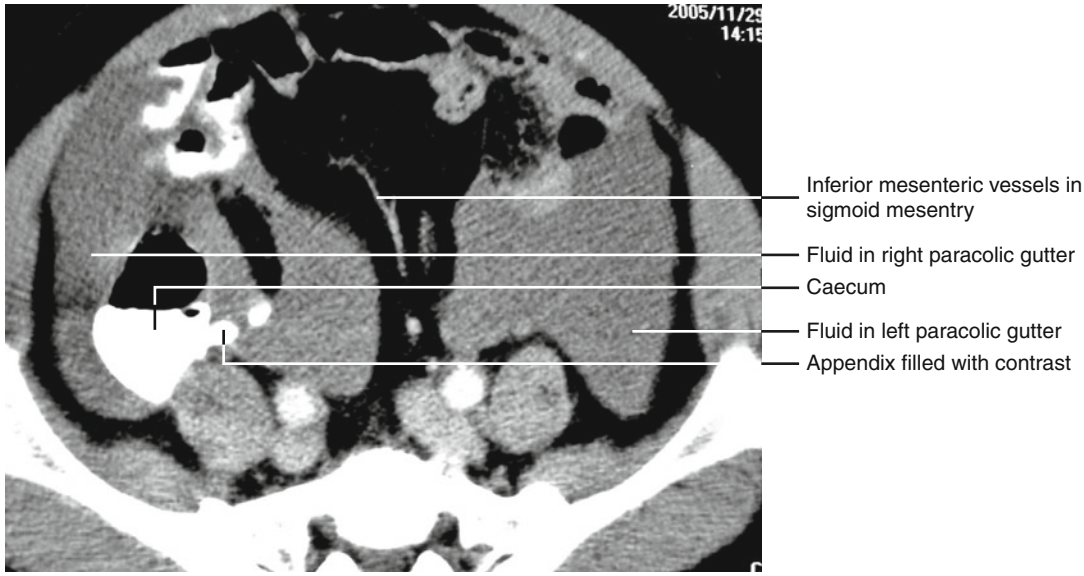

Fig. 21.21 Axial post contrast CT demonstrating the appendix in a patient with ascites

Pearl
The ileocaecal valve can cause a significant filling defect mimicking a soft tissue mass.

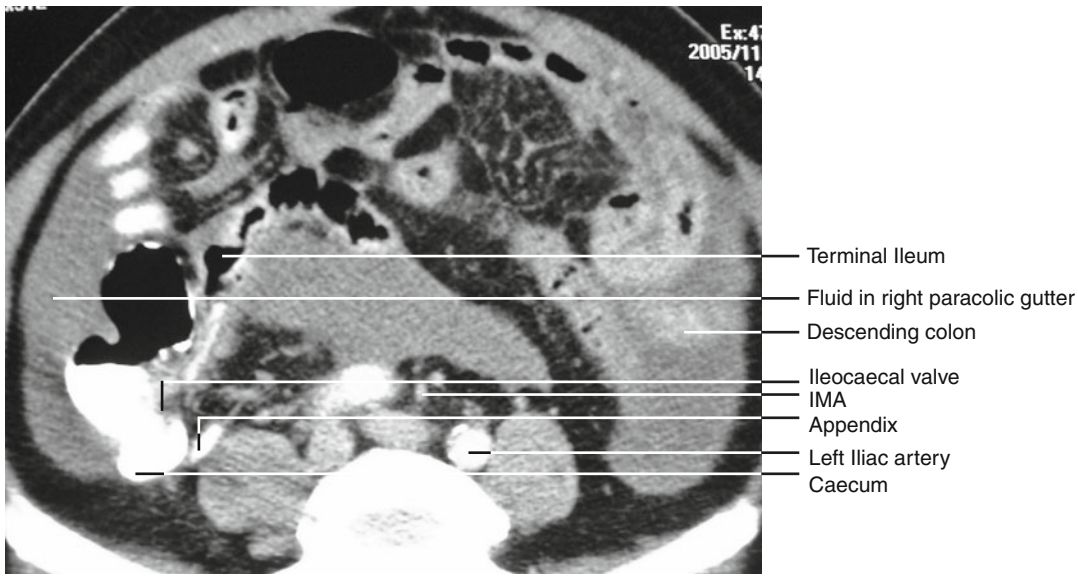

Fig. 21.22 Axial post contrast CT demonstrating the terminal ileum in a patient with ascites

Virtual Colonoscopy

Pearl
Fluid and faecal matter may mimic pathology – hence correlate supine and prone axial CT reference images, with CT virtual colonoscopy images.

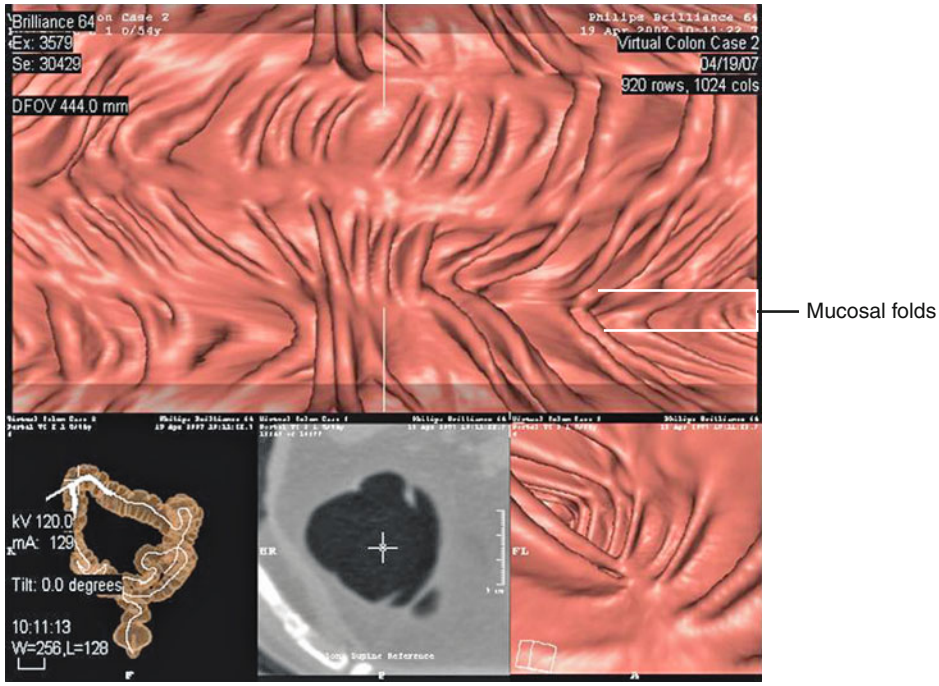

Fig. 21.23 Normal CT virtual colonoscopy. Fillet post processing elongated flattened view of the dissected colon (*top*). Volume-rendered image of the colon in which an automatically central colonic path is created prior to colon virtual dissection (*bottom left*). Axial CT image for reference (*bottom middle*). Virtual endoscopic image (*bottom right*)

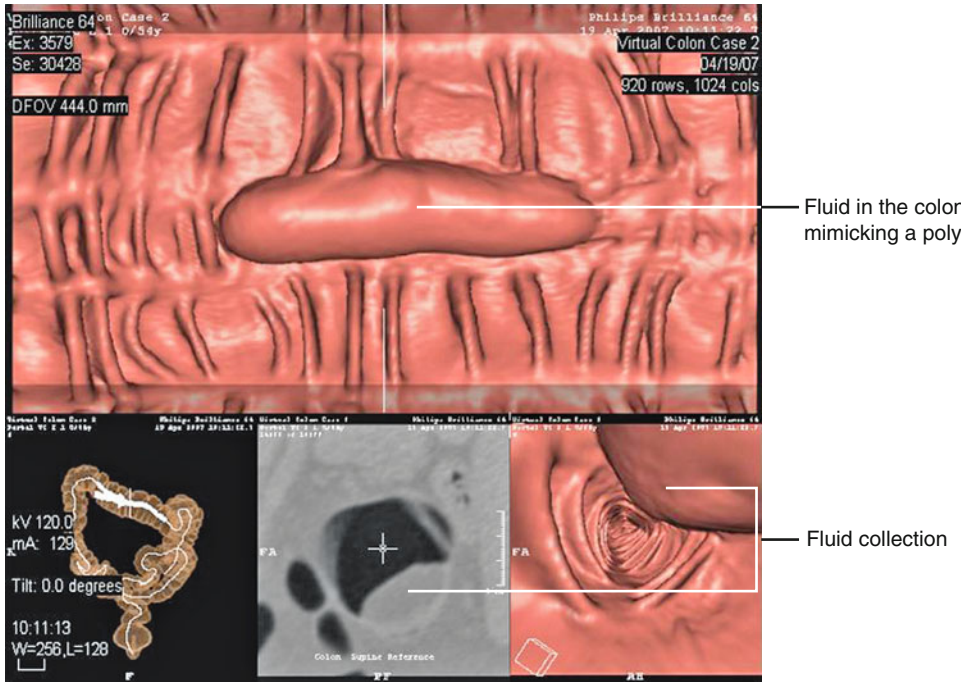

Fig. 21.24 Fluid in colon mimicking a polyp. Fillet view (*top*). Volume-rendered image (*bottom left*). Axial CT reference image (*bottom middle*). Endoscopic image (*bottom right*)

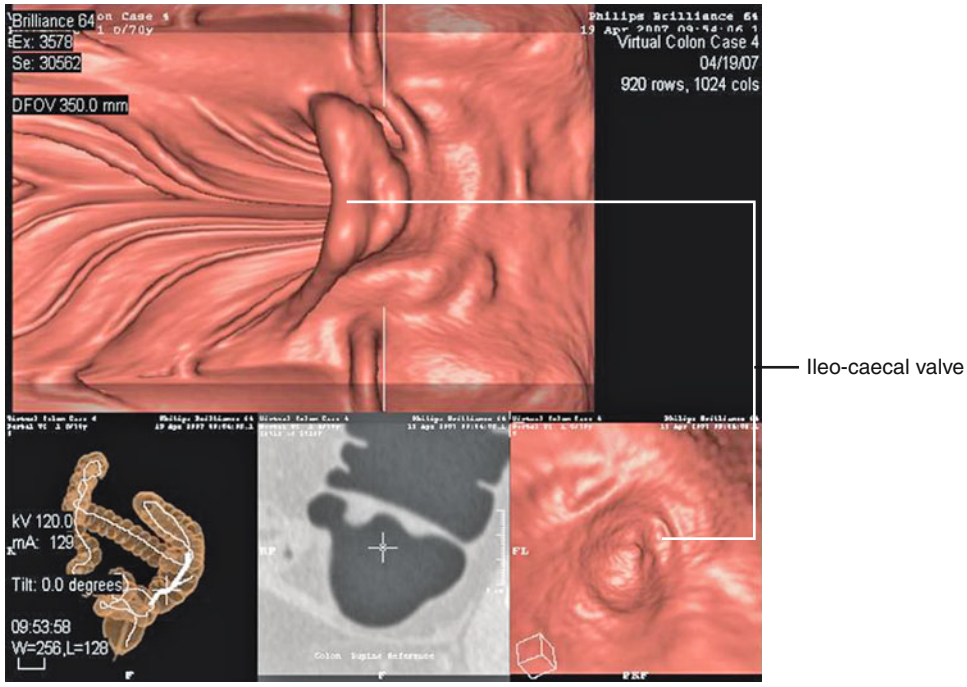

Fig. 21.25 Valve of Bauhini (ileo-caecal valve). CT colonoscopy (*top* and *bottom right*). Axial CT image for reference (*middle*). Prone volume-rendered image of the colon (*bottom left*)

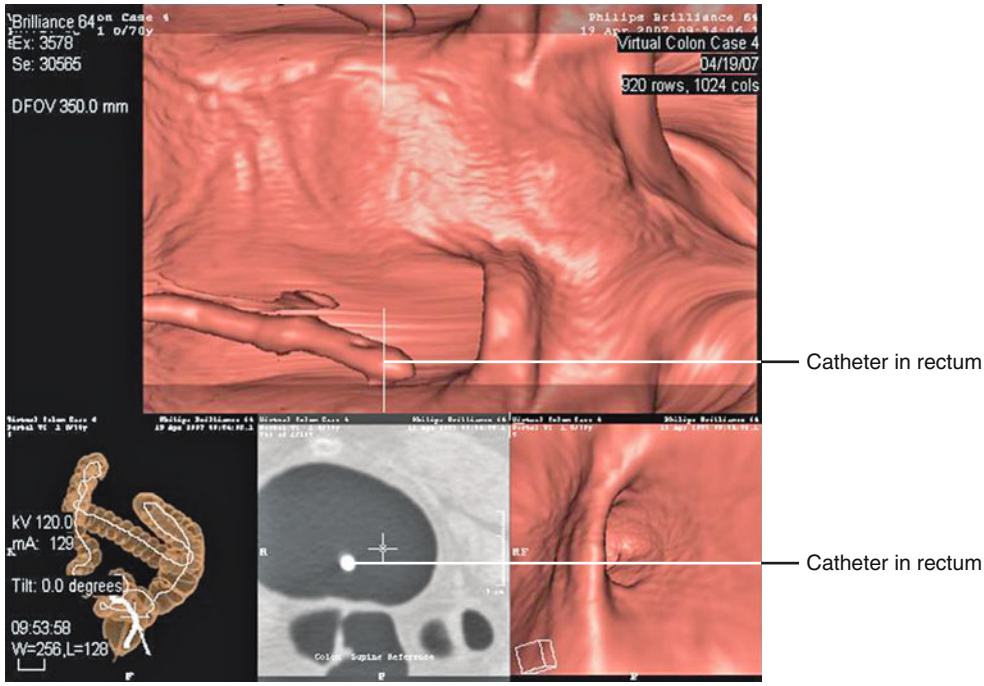

Fig. 21.26 Catheter in the rectum. Fillet view (*top*). Volume-rendered image of the colon in which an automatically central colonic path is created prior to colon virtual dissection (*bottom left*). Axial CT image for reference (*bottom middle*). Virtual endoscopic image (*bottom right*)

Magnetic Resonance Imaging

Demonstrates bowel with similar detail as CT but with additional benefits of better mural and biliary tree assessment.

Optimally demonstrates pelvic floor and anal sphincters.

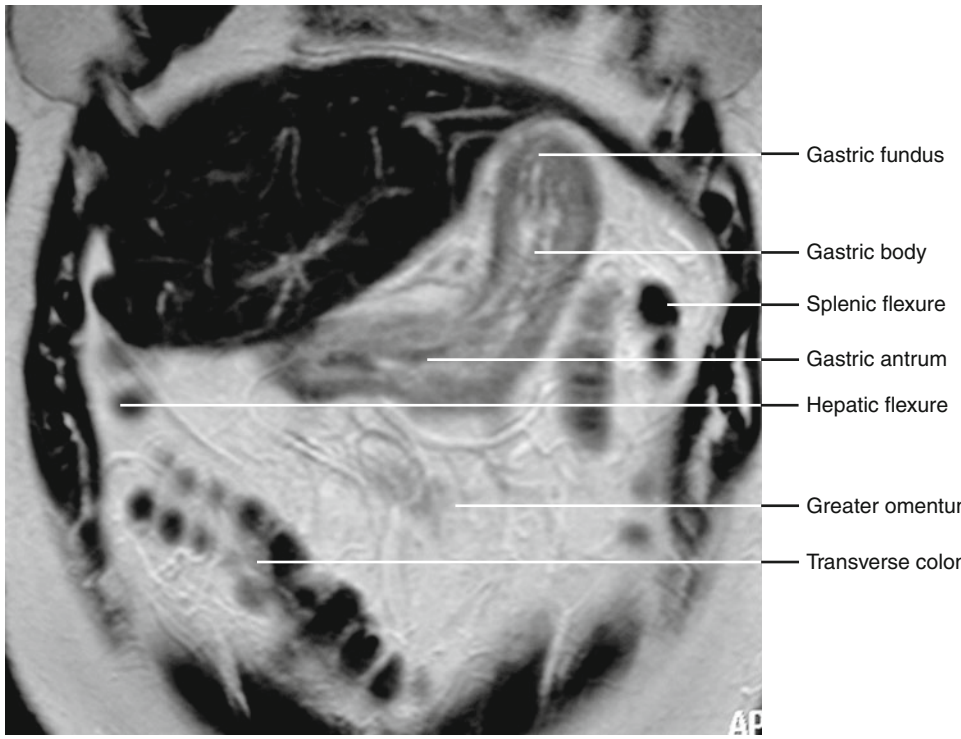

Fig. 21.27 T2 coronal demonstrating the stomach

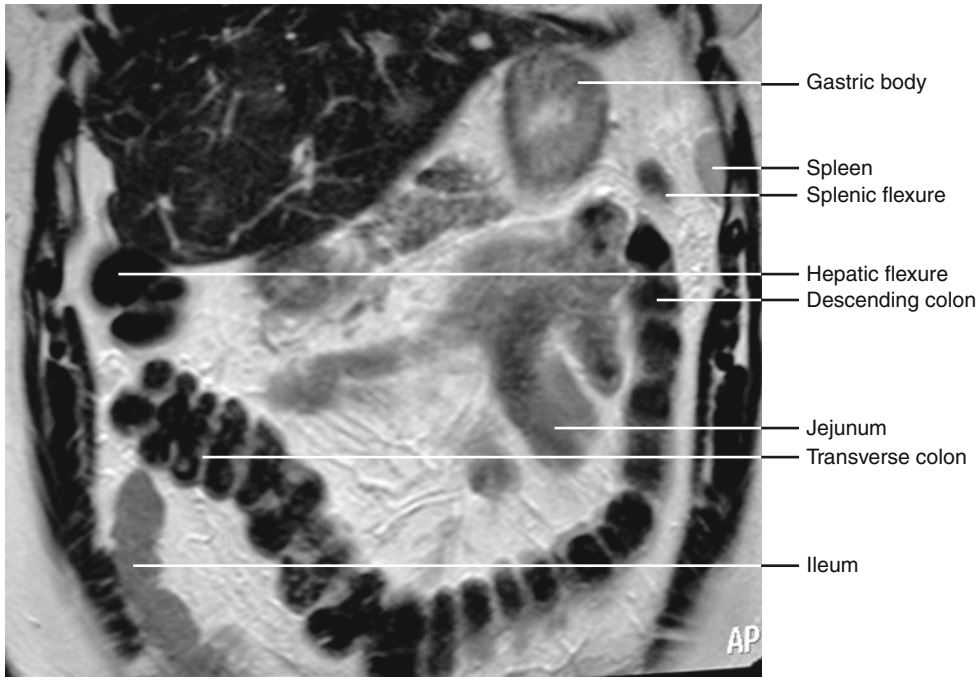

Fig. 21.28 T2 coronal demonstrating the transverse colon

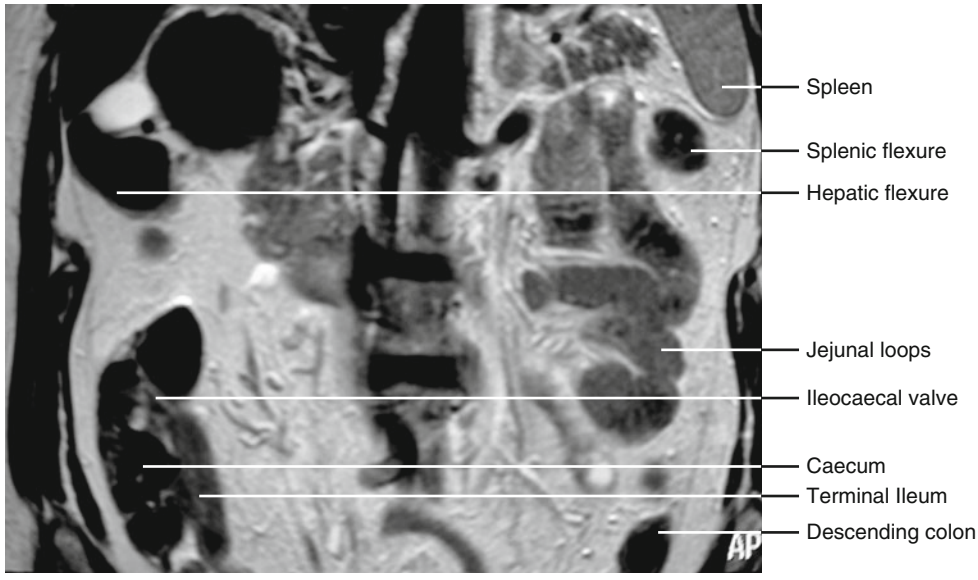

Fig. 21.29 T2 coronal demonstrating the caecum

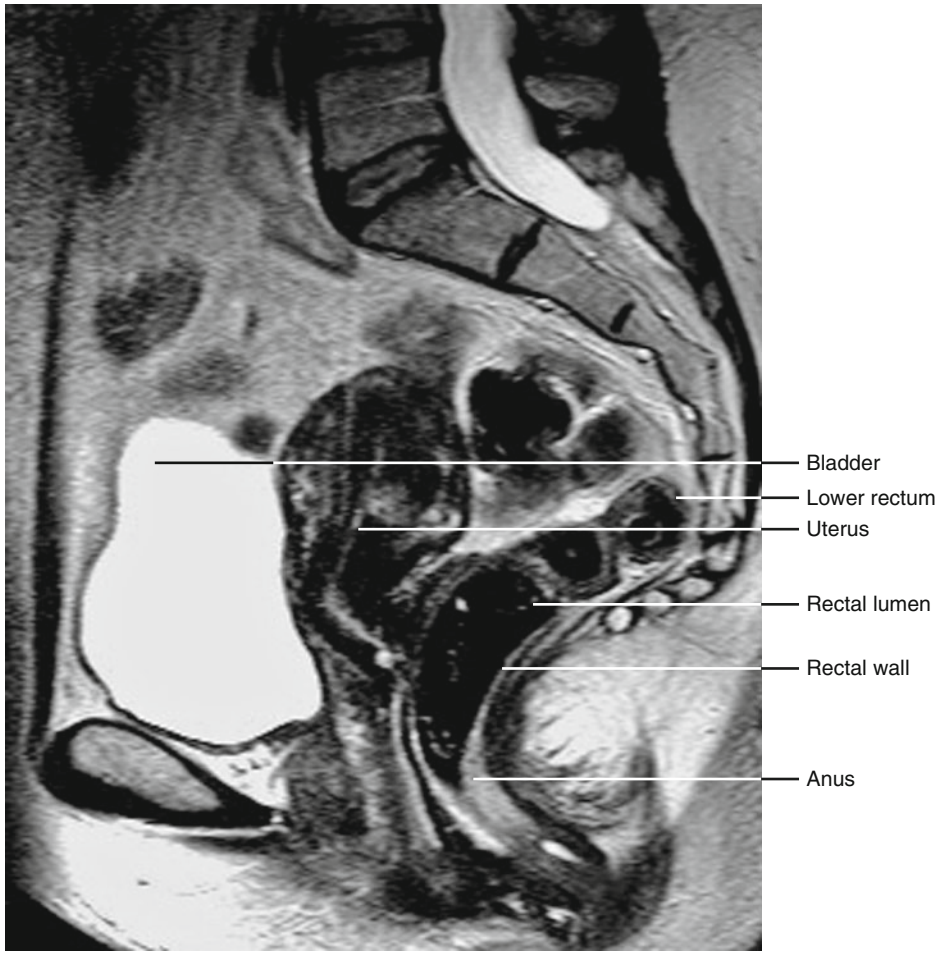

Fig. 21.30 T2 sagittal demonstrating the rectum in a female

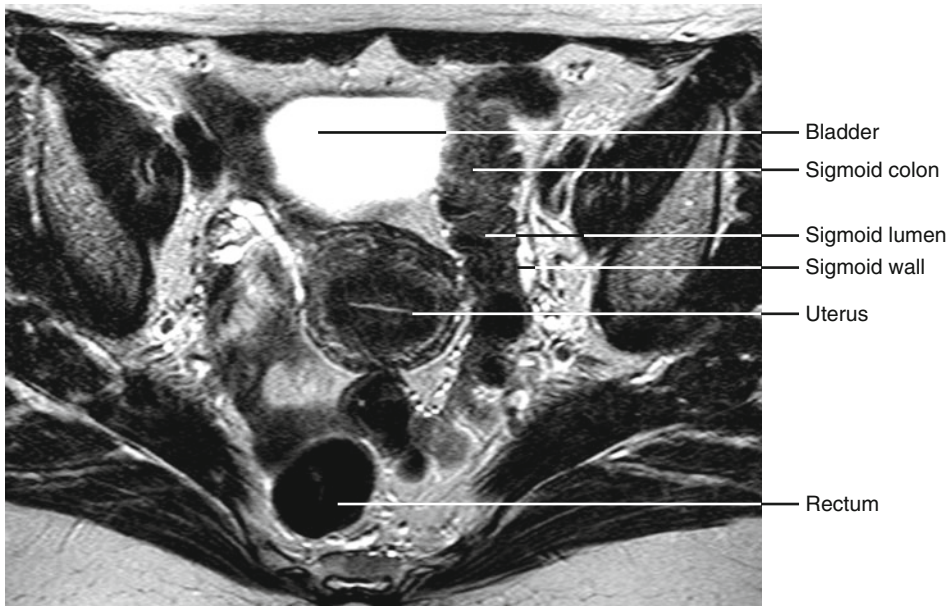

Fig. 21.31 T2 axial demonstrating the rectum in a female

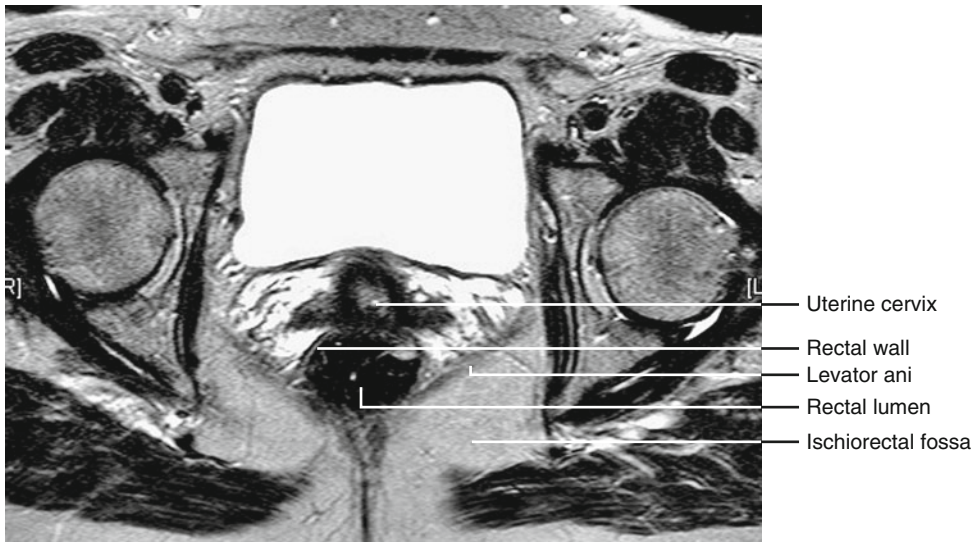

Fig. 21.32 T2 axial demonstrating the rectum in a female

Pearl
The rectal wall consists of:
Mucosa and submucosa: T2 high
Musculari propria: T2 intermediate/high
Perirectal fat: T2 high

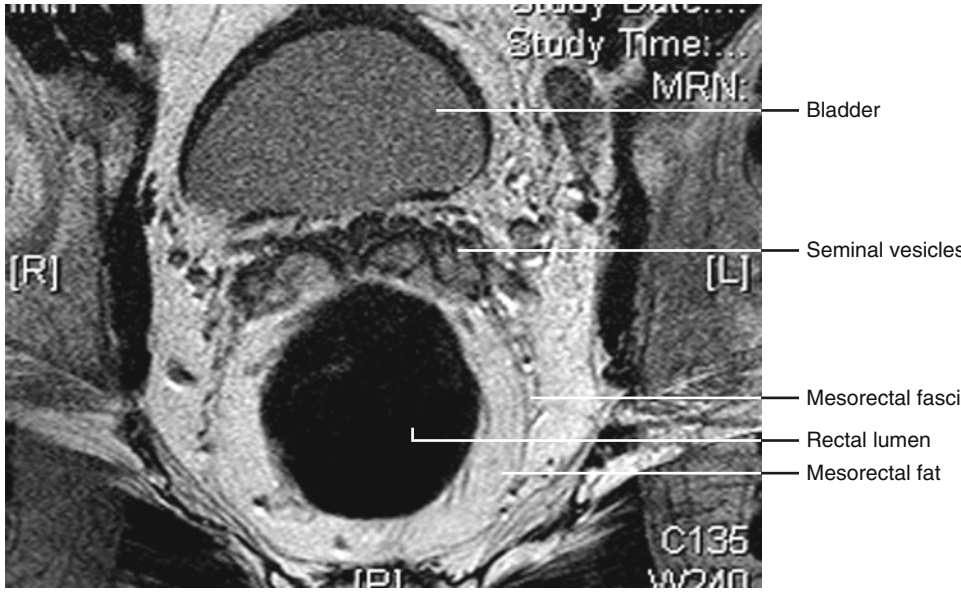

Fig. 21.33 T1 axial demonstrating the rectum in a male

Pearl
The mesorectal space is bounded by the mesorectal fascia surrounding the rectum. It contains fat, lymph nodes, and vessels.

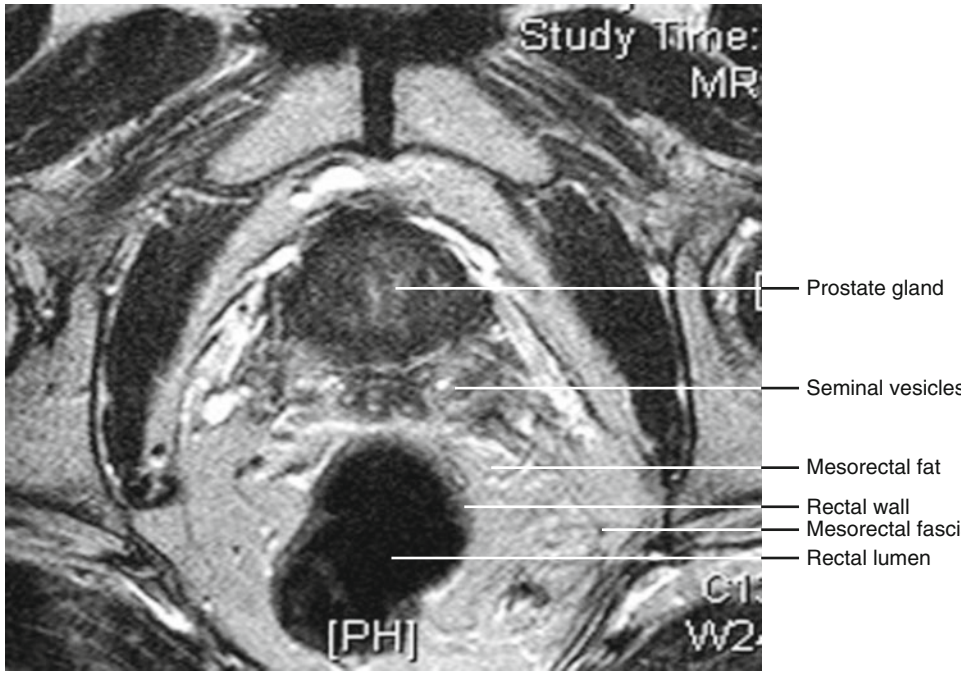

Fig. 21.34 T1 axial demonstrating the rectum in a male

Pearl
The mesorectal fascia blends anteriorly with Devonvillier's fascia of the prostate.

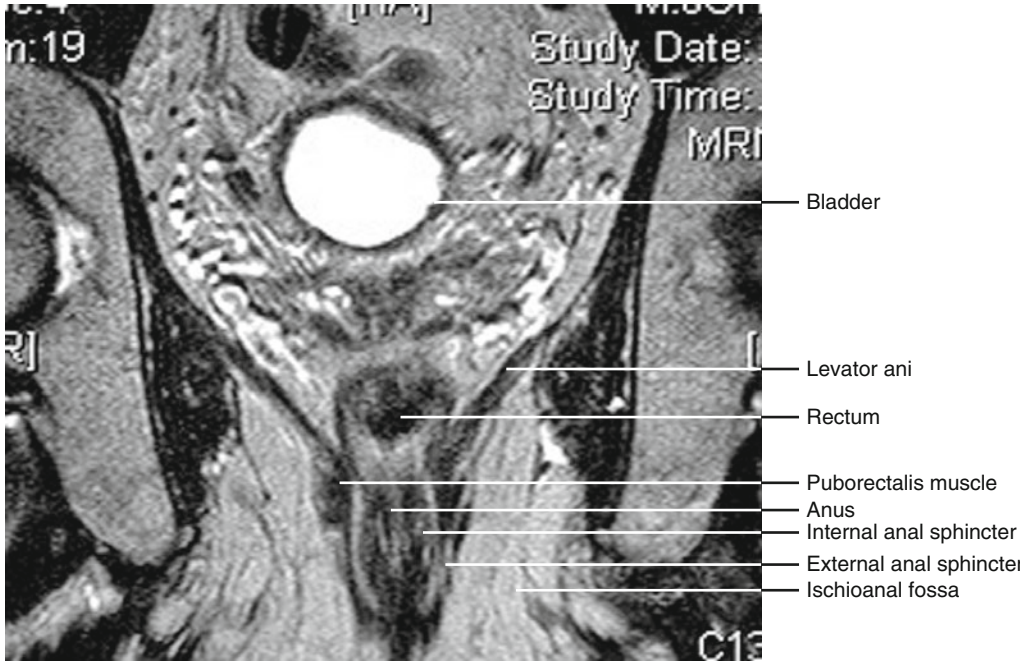

Fig. 21.35 T2 coronal demonstrating the rectum in a male

Pearl
The levator ani muscle is the ceiling of the ischiorectal fossa. Note the rectal wall thickening at the anorectal junction.

Angiography

CT, MR, and catheter angiography are used to assess bowel and visceral blood supply.

Catheter angiography is the gold standard because of better spatial resolution, ability to assess flow dynamics, and intervention in the same setting.

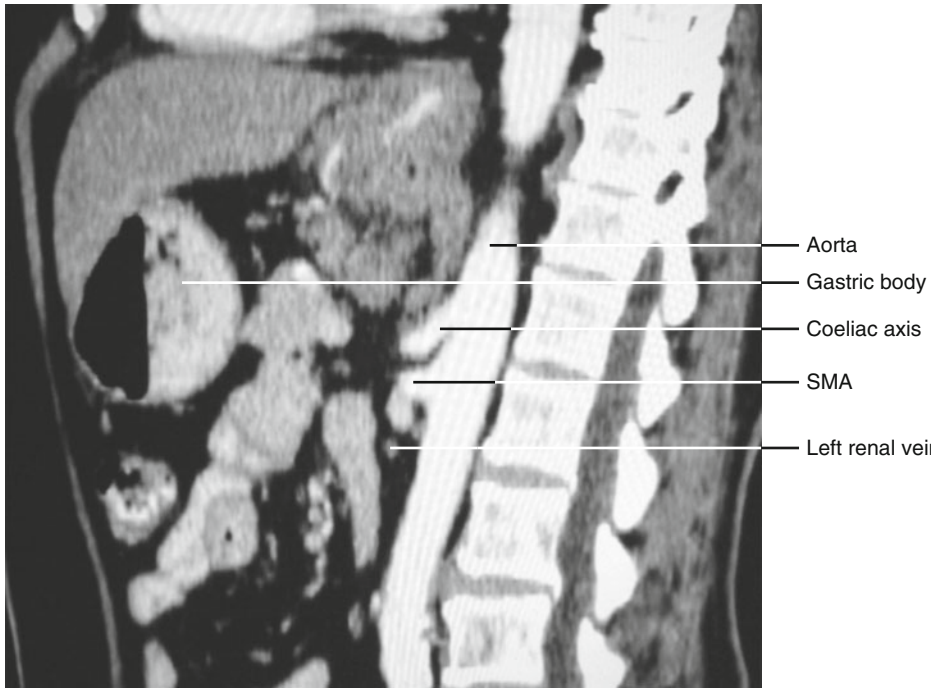

Fig. 21.36 Sagittal CT reconstruction after IV and oral contrast

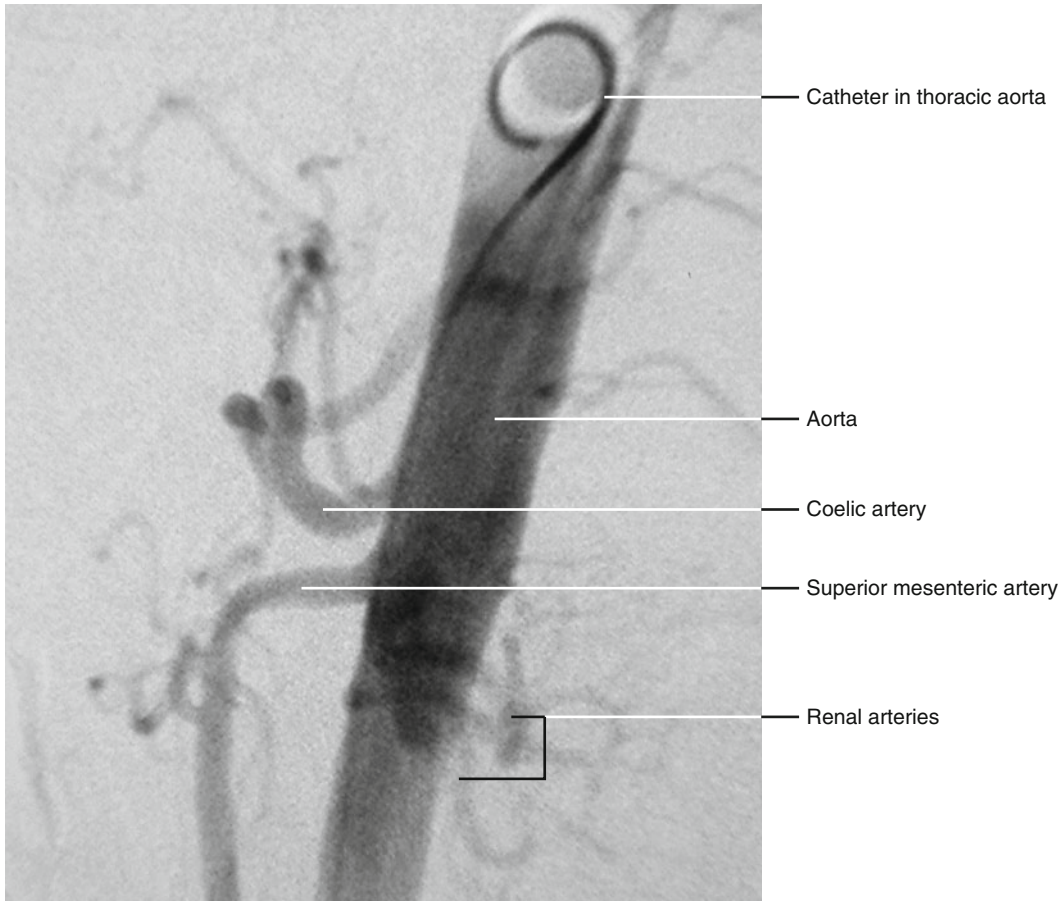

Fig. 21.37 Lateral angiogram of the abdominal aorta

Pearl
The normal angle between the aorta and SMA is 45°–65°.

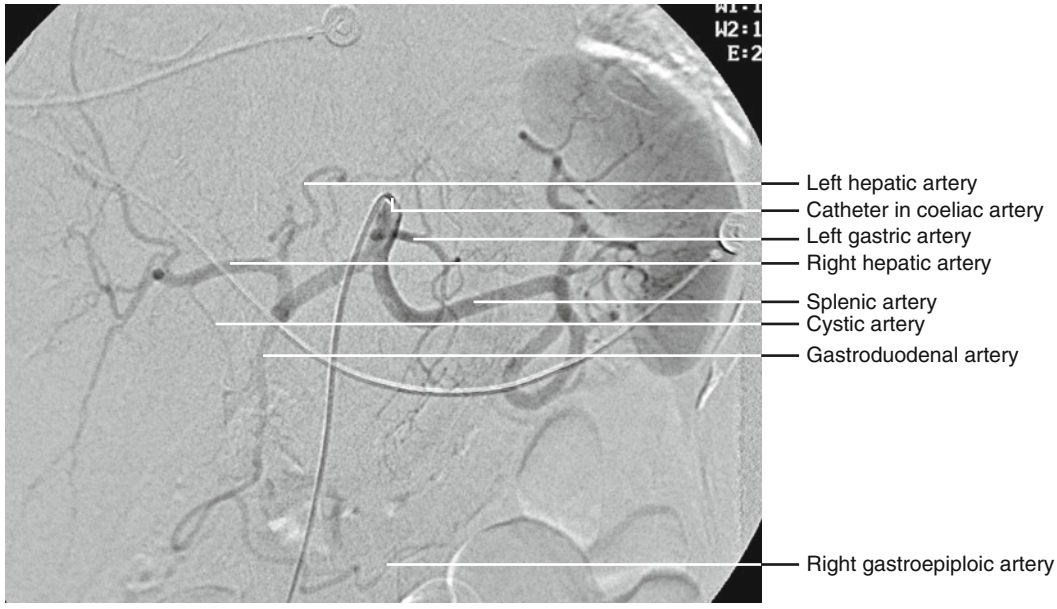

Fig. 21.38 Selective coeliac artery angiogram

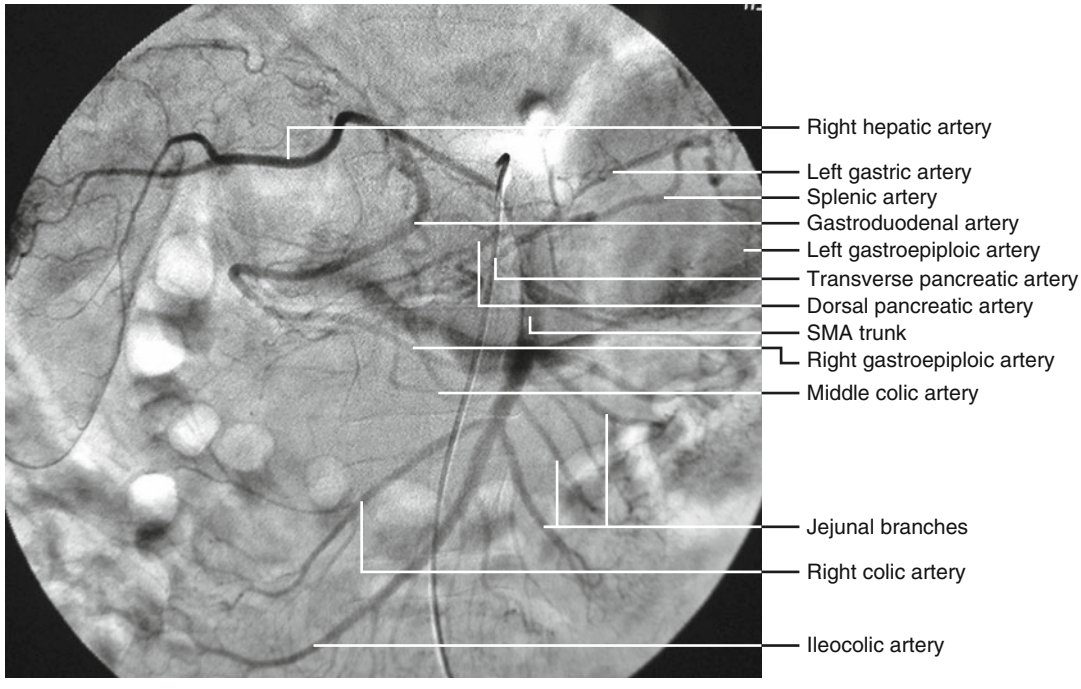

Fig. 21.39 Coeliac and mesenteric artery angiogram

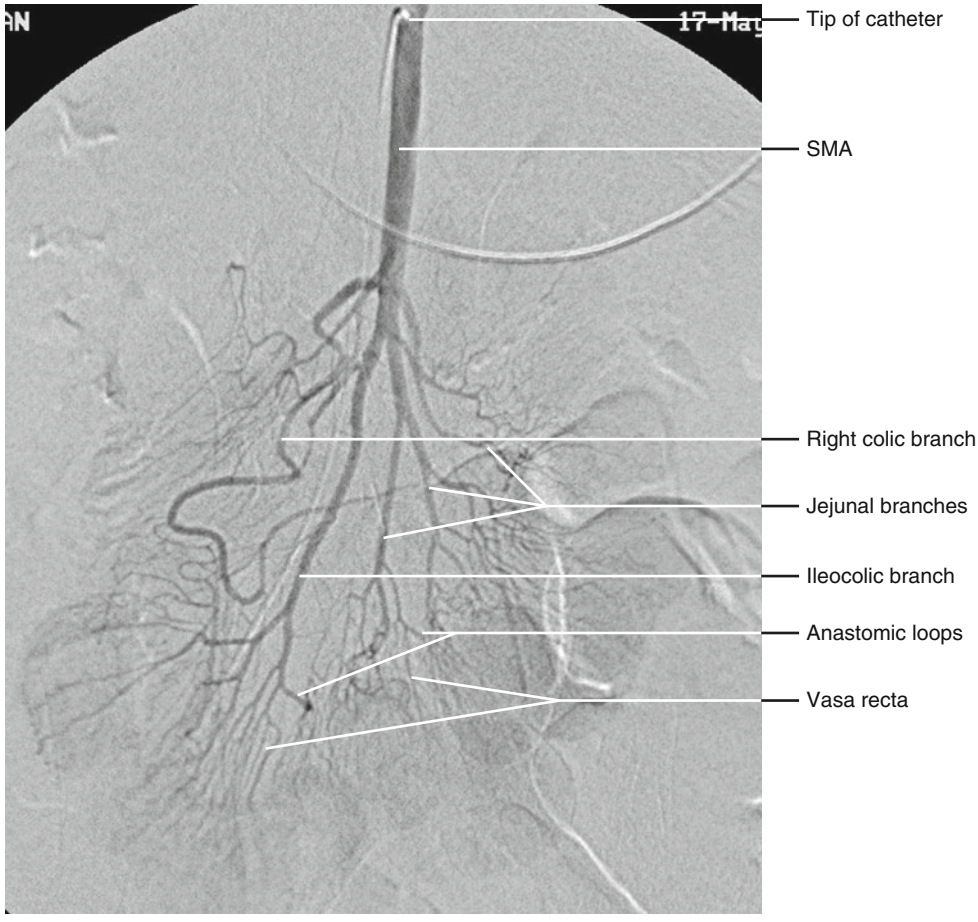

Fig. 21.40 Selective superior mesenteric artery angiogram